THE JOURNAL OF BIOLOGICAL CHEMISTRY VOL. 284, NO. 44, pp. 30129–30137, October 30, 2009

Diversity and Developmental Expression of L-type Calcium Channel β2 Proteins and Their Influence on Calcium Current in Murine Heart*[S]

Received for publication, July 16, 2009, and in revised form, September 1, 2009 Published, JBC Papers in Press, September 1, 2009, DOI 10.1074/jbc.M109.045583

Sabine Link[1], **Marcel Meissner, Brigitte Held**[2], **Andreas Beck, Petra Weissgerber, Marc Freichel, and Veit Flockerzi**[3]
From the Experimentelle und Klinische Pharmakologie und Toxikologie, Universität des Saarlandes, 66421 Homburg, Germany

By now, little is known on L-type calcium channel (LTCC) subunits expressed in mouse heart. We show that CaVβ2 proteins are the major CaVβ components of the LTCC in embryonic and adult mouse heart, but that in embryonic heart CaVβ3 proteins are also detectable. At least two CaVβ2 variants of ~68 and ~72 kDa are expressed. To identify the underlying CaVβ2 variants, cDNA libraries were constructed from poly(A)$^+$ RNA isolated from hearts of 7-day-old and adult mice. Screening identified 60 independent CaVβ2 cDNA clones coding for four types of CaVβ2 proteins only differing in their 5′ sequences. CaVβ2-N1, -N4, and -N5 but not -N3 were identified in isolated cardiomyocytes by RT-PCR and were sufficient to reconstitute the CaVβ2 protein pattern *in vitro*. Significant L-type Ca^{2+} currents (I_{Ca}) were recorded in HEK293 cells after co-expression of CaV1.2 and CaVβ2. Current kinetics were determined by the type of CaVβ2 protein, with the ~72-kDa CaVβ2a-N1 shifting the activation of I_{Ca} significantly to depolarizing potentials compared with the other CaVβ2 variants. Inactivation of I_{Ca} was accelerated by CaVβ2a-N1 and -N4, which also lead to slower activation compared with CaVβ2a-N3 and -N5. In summary, this study reveals the molecular LTCC composition in mouse heart and indicates that expression of various CaVβ2 proteins may be used to adapt the properties of LTCCs to changing myocardial requirements during development and that CaVβ2a-N1-induced changes of I_{Ca} kinetics might be essential in embryonic heart.

Cardiac contractions require Ca^{2+} influx in cardiomyocytes from the extracellular fluid, which leads to Ca^{2+} release from the sarcoplasmic reticulum via ryanodine receptors (1).

This Ca^{2+}-induced Ca^{2+} release (CICR)[4] causes a marked increase in intracellular Ca^{2+} concentration for short periods of time and underlies cardiac contraction (2, 3). The Ca^{2+} influx into cardiac myocytes is mediated by high voltage-activated L-type Ca^{2+} channels (LTCCs), which are heteromultimeric complexes comprised predominantly of the pore-forming CaVα_1 subunit and the auxiliary CaVβ subunit (4). In heart, the principal CaVα_1 subunit, CaVα_1c (CaV1.2), is encoded by the *Cacna1C* gene (5). Four genes (*Cacnb1-4*) encoding CaVβ subunits have been identified that are expressed in the heart of different species including human, rabbit, and rat (6, 7, 8).

CaVβ proteins are ~500 amino acid cytoplasmic proteins that bind to the CaVα_1 I-II intracellular loop (9) and affect channel gating properties (4), trafficking (10, 11), regulation by neurotransmitter receptors through G-protein βγ subunit activation (12), and sensitivity to drugs (13). The CaVβ primary sequence encodes five domains, arranged V1-C1-V2-C2-V3. V1, V2, and V3 are variable domains, whereas C1 and C2 are conserved (14). Structural studies reveal that C1 and C2 form a SH3 domain (Src homology 3 domain) and a NK domain (nucleotide kinase domain), respectively (15). Although C1-V2-C2 makes the CaVβ core, in heart the V1 region appears critical for the kinetics of I_{Ca} and heart function. Accordingly a mutation in the V1 region of the *Cacnb2* gene was recently identified as an underlying cause of Brugada syndrome (16).

In mice-targeted deletion of the *Cacnb2* gene (17) but not of *Cacnb1* (18), *Cacnb3* (19, 20), or *Cacnb4* (21) leads to a morphologically and functionally compromised heart, which causes severe defective remodeling of intra- and extra-embryonic blood vessels and death at early embryonic stages both when the *Cacnb2* gene was targeted globally or in a cardiac myocyte-specific way (17). Although these results point to an essential role of CaVβ2 for I_{Ca} and cardiac function, the existence of various CaVβ2 splice variants and heterogeneity of the expressed CaVβ2 proteins require further studies on the subunit composition of LTCCs in the mouse heart. In addition and in view of the growing number of preclinical studies using mouse models carrying definite Ca^{2+} channel subunits as transgenes in heart tissue, the identification of the relevant gene products underlying the endogenous mouse cardiac L-type channel is essential. Recent mouse models (*e.g.* 22, 23, 24) carrying a rat CaVβ2 splice variant ("rat CaVβ2a") (25) expressed in rat and rabbit brain (26), but not in rabbit heart (26), have only escalated this requirement, because it has never been shown that the mouse orthologue of this variant is endogenously expressed in the mouse heart.

So far, five CaVβ2 variants varying only in the V1 domain have been identified from different species (25, 27, 28) and in

* This work was supported in part by HOMFOR (to M. M. and V. F.), Deutsche Forschungsgemeinschaft and Forschungskommission der Universität des Saarlandes (to V. F.), and Fonds der Chemischen Industrie (to V. F.).
[S] The on-line version of this article (available at http://www.jbc.org) contains supplemental Figs. S1 and S2, data, and Tables S1–S6.
[1] To whom correspondence may be addressed. Tel.: 49-6841-1626400; Fax: 49-6841-1626402; E-mail: sabine.link@uks.eu.
[2] Present address: Institut für Pharmazeutische Chemie, Goethe-Universität Frankfurt, 60438 Frankfurt/Main, Germany.
[3] To whom correspondence may be addressed. Tel.: 49-6841-1626400; Fax: 49-6841-1626402; E-mail: veit.flockerzi@uks.eu.
[4] The abbreviations used are: CICR, Ca^{2+}-induced Ca^{2+} release; CaV, voltage-dependent Ca^{2+} channel; LTCC, L-type calcium channel; SH3, Src homology; NK, nucleotide kinase; V, variable region; C, constant region; E, embryonic day; P, postnatal day; GSP, gene-specific primer.

human heart these variants have been obtained mainly by RT-PCR approaches (29, 30). In contrast, there is little information on the CaVβ proteins present in mouse heart, their respective splice variants, and expression ratios. We therefore started to study CaVβ expression in the murine heart using Western blots and cDNA cloning and to reveal their functional impact on LTCCs formed by the murine CaV1.2 protein.

EXPERIMENTAL PROCEDURES

Antibodies and Western Blot Analysis—Microsomal protein fractions or protein/cell lysates were solubilized with SDS buffer, denatured and subjected to SDS-PAGE and Western blotting. The nitrocellulose membrane (Hybond-C extra, Amersham Biosciences) was probed after transfer with antibodies against CaVβ1, CaVβ2, CaVβ3, CaVβ4, and CaVα1c (CaV1.2) subunits. Polyclonal anti-CaVβ antibodies 234 (CaVβ1b), 424 and 425 (CaVβ2), 828 and MM(CaVβ3), and 830 and 1051 (CaVβ4), which were generated in-house and affinity-purified were used in this study. Specificity of antibodies was confirmed by using microsomal membrane protein fractions from wild type mice and mice deficient in CaVβ2, CaVβ3, and CaVβ4. The anti CaV1.2 antibodies were kindly provided by Dr. Franz Hofmann, Munich.

Northern Blot Analysis—10 μg of murine heart poly(A)$^+$ RNA was resuspended in 50% deionized formamide, 5.92% formaldehyde, 20 mM 4-morpholinepropanesulfonic acid, 2 mM sodium acetate, 1 mM EDTA, and 0.5 μg/μl ethidium bromide. After incubation at 55 °C for 15 min, samples were put on ice and deionized formamide, bromphenol blue, xylene cyanol, and 5 mM EDTA were added at final concentrations of 15.8%, 0.42%, 0.42%, and 0.83 mM, respectively. The RNA was electrophoresed on a 1.2% agarose gel containing 1.1% formaldehyde, transferred thereafter to Hybond N nylon membranes (Amersham Biosciences) by diffusion overnight and UV cross-linked to the filters. Membranes were prehybridized for 3 h in 450 mM sodium chloride, 45 mM sodium citrate, 0.2% Ficoll, 0.2% polyvinylpyrrolidone, 0.2% bovine serum albumin, and 150 μg/ml denatured salmon sperm DNA. The membrane was hybridized overnight with random-primed [^{32}P]dCTP-labeled probe (10^7 cpm/μl) in hybridization solution. After four washing steps with 75 mM sodium chloride, 7.5 mM sodium citrate, 0.1% SDS, the membrane was exposed to x-ray films.

Construction and Screening of cDNA Libraries—Murine total RNA was isolated from 695 mg (postnatal day 7 (P7)) or 750 mg (adult, >8 weeks) heart tissue using RNAGold (peqlab). Reverse transcription was performed with 5 μg of poly(A)$^+$ RNA from adult or P7 mouse heart using a CaVβ2 gene specific primer (GSP, 5′-GGA GTG TGC TCT GTC) or hexameric random primers and the Superscript™ Plasmid System with Gateway Technology for cDNA Synthesis and Cloning (Invitrogen). cDNA libraries were constructed in pcDNAII (Invitrogen) and transformed into ElectroMAX™ DH10B™ cells. Bacteria were grown on Duralon-UV nylon membranes (Stratagene). 5×10^5 recombinant clones were screened with radioactive cDNA probes covering the conserved C1 and C2 regions of CaVβ2 (C1 431 bp, exons 3–6; C2 591 bp, exons 8–13). After 3 h of prehybridization, hybridization was carried out overnight at 55 °C for random-primed and at 60 °C for gene-specific primed libraries, respectively. Prehybridization and hybridization solution contained 450 mM sodium chloride, 45 mM sodium citrate, 0.2% Ficoll, 0.2% polyvinylpyrrolidone, 0.2% bovine serum albumin, and 150 μg/ml denatured salmon sperm DNA, with the hybridization solution containing random primed [^{32}P]dCTP-labeled probe (10^5 cpm/μl). After washing steps with solutions containing decreasing concentrations of sodium chloride (450 to 45 mM) and sodium citrate (45 to 4.5 mM), 0.1% SDS, membranes were exposed to x-ray films for 8 and 16 h, respectively. Positive clones were isolated and sequenced.

Isolation of Murine Cardiomyocytes—Embryonic and adult cardiomyocytes were isolated as described before (17, 31).

RT-PCR—For RT-PCR, we used the Superscript™ One Step RT-PCR with Platinum Taq System (Invitrogen). 10–12 cardiomyocytes were selected by patch pipette, pooled in Eppendorf tubes, and directly used for reverse transcription and PCR. CaVβ2-N-specific forward primers (N1, 5′-ATG GTC CAA AGC GAC ACG TC; N3, 5′-ATG CAG TGC TGC GGG CTG; N4, 5′-ATG CTT GAC AGG CAG TTG GTG; N5, 5′-ATG AAG GCC ACC TGG ATC AG) and the common reverse primer (5′-CTC TCT GTT CGT GCT GTA GC) were used. Positive controls were done in the presence of 5 ng of the respective CaVβ2a-N plasmid used as template, negative controls in the presence of H_2O instead of template; reactions were performed in parallel. PCR (39 cycles) conditions were: reverse transcription at 50 °C for 25 min, one denaturation step at 94 °C for 2 min to inactivate the reverse transcriptase and to activate PCR polymerase, denaturation at 94 °C for 30 s, annealing at 57 °C for 30 s and extension at 72 °C for 35 s.

Cell Culture and Transfection—HEK293 cells and COS cells were grown in MEM and Dulbecco's modified Eagle's medium (Invitrogen), respectively, supplemented with 10% fetal calf serum (Invitrogen) and maintained under standard cell culture conditions (37 °C, 5% CO_2).

COS cells were transiently co-transfected with 2 μg of CaVβ2 cDNA-encoding plasmids. HEK293 cells were transiently co-transfected with 0.7 μg full-length CaV1.2 subunit together with 0.7 μg of the different murine cardiac CaVβ2 cDNA encoding plasmids and 0.7 μg eGFP. Transfection was carried out with Fugene6 (Roche Applied Sciences). Electrophysiological recordings in GFP-positive cells were obtained 48–72 h after transfection.

Electrophysiological Recordings—For whole-cell Ca^{2+} current recordings, HEK293 cells expressing CaV1.2 and CaVβ2 were bathed in a solution containing (in mM): tetraethylammonium chloride 140, $MgCl_2$ 1, $CaCl_2$ 1.8, HEPES 10, pH 7.4 (TEA-OH). Borosilicate patch pipettes (BioMedical Instruments) were filled with a solution containing (in mM): CsCl 120, $MgCl_2$ 3, Mg-ATP 5, EGTA 10, HEPES 5, pH 7.4 (CsOH), and had resistances ranging from 2.0 to 4.0 MΩ. Currents were filtered at 1.67 kHz and digitized at a 5-kHz interval. I_{Ca} was normalized to cell size. Currents were activated from the holding potential of K90 mV every 5 s by step depolarizations from −70 to +70 mV in 10 mV increments for 400 ms to obtain current-voltage (I-V) relationships. In some HEK293 cells just transfected with CaV1.2 and GFP lacking CaVβ2, a small but clear I_{Ca} could be discerned (maximal I_{Ca} at 0 mV −2.23 pA/pF,

$n = 24$). Therefore only cells transfected with CaV1.2 and one of the CaVβ2 isoforms, with a current density larger than −3.5 pA/pF at 0 mV were included in the analysis to ensure that both transfected proteins CaV1.2 and CaVβ2 were present. Current-voltage (I-V) relationships from individual cells were fitted with $I = G_{max}(V\text{-}E_{rev})/(1 + \exp(-(V\text{-}V_{1/2,act})/k))$ (32), where G_{max} represents the whole-cell conductance, E_{rev} the apparent reversal potential, $V_{1/2,act}$ the voltage for half-maximal activation of the current and k the slope factor. The time to peak was measured 1.2 ms after the beginning of the depolarization to avoid measuring capacitance artifacts. The steady-state activation curve was constructed by normalizing the current density measured between −70 mV and 0 mV to that at 0 mV and fitted with a Boltzman equation $I/I_{0mV} = 1 + (A\text{-}1)/(1 + \exp((V\text{-}V_{1/2,ss\text{-}act})/k))$, with $V_{1/2,ss\text{-}act}$ as the voltage of half-activation, k the slope factor. Steady-state inactivation was measured by a double-pulse protocol; cells were depolarized from a holding potential of −90 mV to potentials from −100 to +40 mV for 5 s in 10-mV increments; subsequently the test pulse to 0 mV for 400 ms was applied. Steady-state inactivation curves were normalized to the current after the prepulse to −100 mV, averaged, and fitted with a Boltzman equation $I/I_{max} = 1/(1 + \exp((V\text{-}V_{1/2,inact})/k)$ with $V_{1/2,ss\text{-}inact}$ as the voltage of half-inactivation and k the slope factor. Voltage protocols were applied, and currents recorded with an EPC9 patch-clamp amplifier (HEKA, Germany) controlled by the software PulseFit (HEKA). A P/4 protocol was used in all experiments to subtract linear leak and capacitance. Data were compared in GraphPad Prism using a one-way analysis of variance test.

RESULTS

CaVβ Protein Expression in Adult Heart and Brain from Mice

We made use of specific antibodies for CaVβ1, CaVβ2, CaVβ3, and CaVβ4 to detect the CaVβ subunits in protein fractions from adult mouse heart and brain by Western blot. The CaVβ1, CaVβ3, and CaVβ4 proteins are readily detectable in adult brain (Fig. 1*A*, 75 μg of protein per lane) but not in the adult heart although 200 μg of cardiac proteins were applied per lane. In contrast, the CaVβ2 protein is detected in brain (75 μg of protein per lane) and in heart (15 μg of cardiac protein was applied per lane), demonstrating that CaVβ2 is the predominant CaVβ protein in the adult mouse heart. Accordingly transcripts of the *Cacnb2* gene of ~2, ~3.5, ~4, and ~5 kb are readily detectable in poly(A)$^+$ RNA isolated from adult mouse heart (Fig. 1*B*).

CaVβ2 Protein Expression in Developing Mouse Hearts

The CaVβ2 protein is detectable in the developing heart tube approximately at embryonic day (E)8.5. To study its expression during cardiac development, immunoblots with protein fractions prepared from hearts from E10.5 to E17.5, neonatal mice (P1), P7, and adult mouse hearts were analyzed for CaVβ2, CaVβ3, and the CaVα_1c subunit expression. In early embryonic heart, a ~72-kDa CaVβ2 protein is expressed (Fig. 1*C*). Interestingly, the CaVβ2 protein detected in brain lysate shares molecular weight with this embryonic ~72-kDa CaVβ2 protein (Fig. 1*C*). In later stages of embryonic development a second CaVβ2 protein of ~68 kDa is co-expressed, whereas in the adult heart only the ~68-kDa CaVβ2 protein (Fig. 1, *A* and *C*) but not the ~72-kDa protein is detectable. The ~55-kDa CaVβ3 protein, which is expressed in brain (Fig. 1, *A* and *D*) is detectable to a very minor degree in the protein fractions from embryonic heart but not in adult heart (Fig. 1, *A* and *D*) whereas the expression of the CaVα_1c proteins parallels CaVβ2 protein expression during cardiac development (Fig. 1*C*). Apparently, different CaVβ2 proteins are expressed during cardiac development leading to changes in LTCC protein composition. The CaVβ3 protein is primarily expressed in brain (Fig. 1, *A* and *D*) but also in heart at early embryonic stages (Fig. 1*D*). Immunoblots clearly show expression of CaVβ3 in heart lysates from wild type mice at E12.5 and E14.5 but not in lysates of hearts from CaVβ3-deficient mice (Fig. 1*D*, CaVβ3$^{-/-}$). However, CaVα_1c and CaVβ2 subunits are the main constituents of embryonic and adult murine cardiac LTCC channels.

The molecular basis of the different CaVβ2 proteins detected by Western blot analysis is not known but could be caused by the expression of splice variants of the *Cacnb2* gene, which has been described in human, rabbit, and rat heart (7, 29, 33). In the

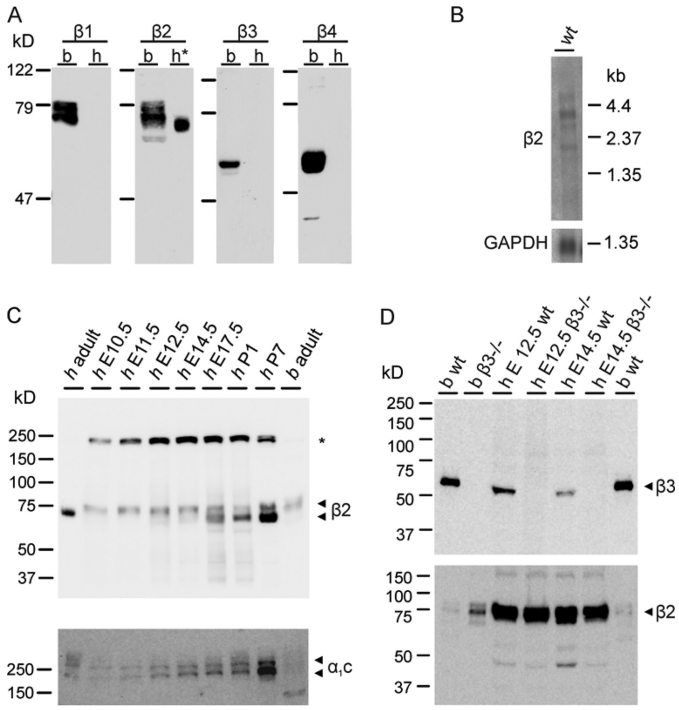

FIGURE 1. **CaVβ2 expression in murine heart and brain.** *A*, immunoblots of microsomal protein fractions from adult mouse heart (*h*, 200 μg per lane; *h**, 15 μg per lane) and brain (*b*, 75 μg per lane) using antibodies for CaVβ1b (β1), CaVβ2 (β2), CaVβ3 (β3), and CaVβ4 (β4). *B*, Northern blot: CaVβ2 transcript expression in 10 μg of poly(A)$^+$ RNA from adult mouse heart probed with a ^{32}P-labeled DNA derived from nucleotides 577–721 of CaVβ2 (GenBank™ Acc. No. L20343). *C*, expression of CaVβ2 (β2) and Cav1.2 (α_1c) during mouse heart development. Immunoblot of microsomal proteins from adult heart (*h adult*, 25 μg) and brain (*b adult*, 50 μg) and lysates of hearts (*h*) taken at embryonic day (*E*) 10.5, 11.5, 12.5, 14.5, 17.5, 1 day (P1), and 7 days (P7) *post partum* and antibodies for CaVβ2 and CaV1.2 as indicated. * indicates myosin, which is present in protein lysates and recognized by the CaVβ2 antibodies; it is not detectable in microsomal protein fractions, which were obtained after differential centrifugation. *D*, expression of CaVβ3 in embryonic heart. Immunoblot of heart protein lysates (150 μg per lane) taken at E12.5 and E14.5 from wild type and CaVβ3-deficient mice. Brain microsomal membrane proteins (20 μg) from wild type and CaVβ3-deficient mice were used as controls. The blot was stripped thereafter and incubated in the presence of the antibody for CaVβ2 to control loading.

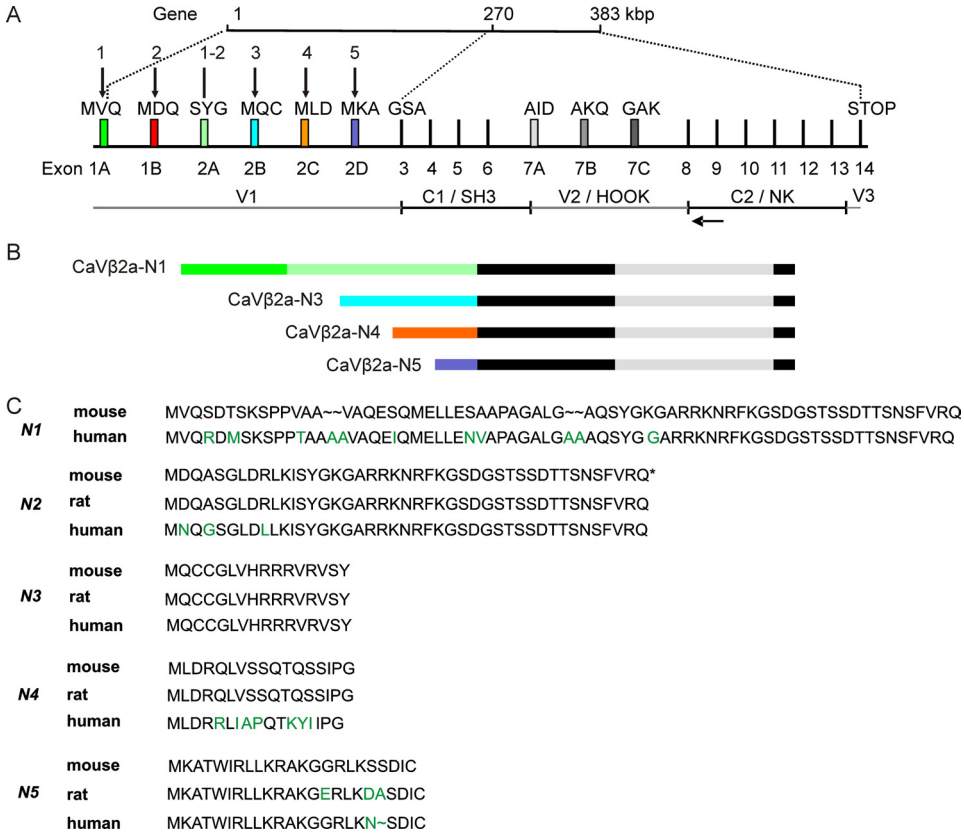

FIGURE 2. **Structure of the mouse *Cacnb2* gene and the various N-terminal V1 domains of CaVβ2 splice variants.** *A*, scheme of the murine *Cacnb2* gene, which is localized on chromosome 2 and comprises 20 protein coding exons. The six exons 1A, 1B, 2A, 2B, 2C, and 2D encode for alternate V1 regions and are scattered among the 5′ 270 kbp. The five domains V1-C1 (SH3, Src homology domain), -V2 (hook domain), - C2 (NK, nucleotide kinase domain), -V3 common to all CaVβ proteins, and their CaVβ2 coding exons are indicated. *M* of exons 1A, 1B, 2B, 2C, and 2D indicate the initiation methionine of CaVβ2 variants CaVβ2a-N1 (1A plus 2A), -N2 (1B plus 2A), -N3 (2B), -N4 (2C), and -N5 (2D), and STOP the common termination. *Arrow* indicates GSP, gene-specific primer, which is complementary to C2 and used to specifically prime the cDNA libraries. *B*, scheme of the four CaVβ2 variants identified in murine heart; they differ in V1, but not in C1 (starting with amino acids GSA), V2 (exon 7A), C2, and V3. Colors of V1 correspond to colors of coding exons. 34 of 60 independent clones coded for CaVβ2a-N4, 16 for CaVβ2a-N1, five for CaVβ2a-N5, and one for CaVβ2a-N3. *C*, amino acid alignment of the V1 domains of CaVβ2 from mouse (this study), rat and human; from the mouse sequences differing amino acids are highlighted in *green*; ~, no amino acid residue; * predicted sequence. GenBank™ accession numbers: N1 mouse BC109156, this study FM872408; N1 human AF423191; N2 mouse predicted from genomic sequence; N2 rat AY190119; N2 human AF423190; N3 mouse this study FM872406; N3 rat NM_053851; N3 human AF423189; N4 mouse this study AM259383; N4 rat AF_423193; N4 human NM_201590; N5 mouse L20343, this study FM872407; N5 rat AY190120; N5 human NM_201570.

following we identified and characterized CaVβ2 variants in mouse heart by the unbiased approach of constructing and screening of cDNA libraries.

Structure of the Cacnb2 Gene, Strategy to Construct cDNA Libraries, and Isolation of CaVβ2 Variants

The murine *Cacnb2* gene is localized on chromosome 2, comprises 20 protein coding exons and extends over a region of ~383 kbp. The six 5′ exons 1A, 1B, 2A, 2B, 2C, and 2D (nomenclature according to the human *Cacnb2* gene by Foell *et al.* (29)) encode for alternate V1 regions and are scattered among the 5′ ~270 kbp of the gene (Fig. 2*A*). The alternate V2 regions are encoded by the mutually exclusive exons 7A, 7B, and 7C. No splicing events of CaVβ2 V3 region have been described so far. Splicing of V1 and V2 regions could be responsible for the CaVβ2 protein pattern detected in Fig. 1*C*.

To get hold of all CaVβ2 V1 and V2 splice variants expressed in murine heart we used the following strategies. Poly(A)$^+$ RNA was isolated from hearts taken from adult animals and from P7 animals; in the latter, the ~68-kDa- and ~72-kDa CaVβ2 proteins are co-expressed (Fig. 1*C*). We used these RNAs and two types of primers for construction of cDNA libraries: To obtain the nucleotide sequences of the V1 and V2 regions, for which splicing events were most probably expected, the cDNA first strand was primed by oligonucleotides complementary to the 5′-end of the C2 domain, and cDNA library screening was done by a probe covering the C1 domain. Second, we constructed a random-primed cDNA library using the poly(A)$^+$ RNA from P7 hearts, which was screened with probes covering the nucleotides encoding the C1 and the C2 domains. The latter approach should identify CaVβ2 variants with differing C1, C2, or V3 domains.

Altogether 60 independent cDNA clones were isolated from the three libraries and sequenced. The majority of clones encoded the sequences of the V1 and V2 regions of CaVβ2 (Fig. 2 and supplemental Table S1). The random-primed clones also contained the C2 and V3 domains. The V2 domain was encoded in all clones by exon 7A (Fig. 2, *A* and *B*). According to the nomenclature of Foell *et al.* (29), these clones are of the CaVβ2a type (a for the A-type exon 7). Differences were only observed within the V1 domain which gave rise to N termini of type N1 (exons 1A plus 2A), N3 (exon 2B), N4 (exon 2C), and N5 (exon 2D) (Fig. 2). 38 out of the 60 sequenced clones encoded the CaVβ2a-N4 variant, demonstrating that this variant is the predominant CaVβ2a variant in hearts from adult and 7-day-old mice. The CaVβ2a-N5 (5 clones out of 60) and CaVβ2a-N1 variants (16 clones out of 60) are expressed to an intermediate extent. The CaVβ2a-N3 splice variant was only detected once among the 60 CaVβ2 cDNA clones indicating that this variant is only present in a very minor fraction of cardiac LTCCs if at all. The N3-type N terminus is encoded by exon 2B and the corresponding mouse, human, and rat amino acid sequences of this exon are identical and start with ^{1}Met-Gln-Cys-Cys (Fig. 2*C*). The cysteine residues at position 3 and 4 in the N3 terminus of the rat protein have been identified as sites of palmitoylation (34). No N2-type N terminus-encoding

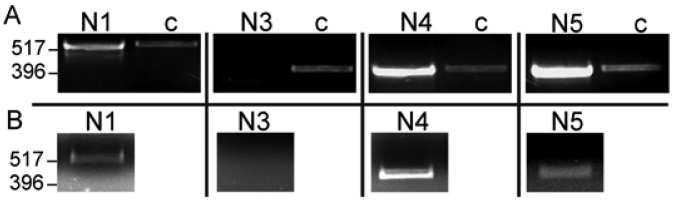

C

	N1	N3	N4	N5
Adult cardiomyocytes	+	-	+	+
Embryonic cardiomyocytes	+	-	+	+

FIGURE 3. **CaVβ2 variant expression in cardiomyocytes.** RT-PCR analysis of the expression of CaVβ2-N transcripts in isolated adult cardiomyocytes (*A*) and isolated embryonic cardiomyocytes (E13.5) (*B*); *c*, control, indicates 5 ng of the respective CaVβ2a-N-plasmid used as template. *C*, summary.

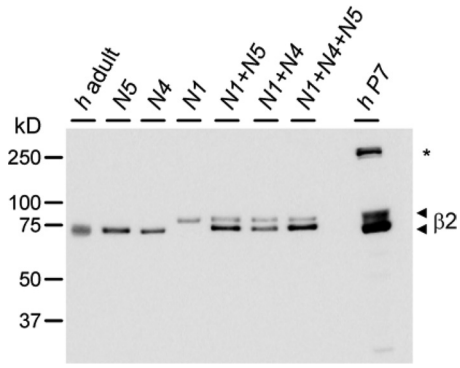

FIGURE 4. ***In vitro* reconstitution of the *in vivo* CaVβ2 protein pattern.** Immunoblot of COS cell lysates expressing the mouse CaVβ2 variants CaVβ2a-N5, -N4, -N1, -N1 plus -N5, -N1 plus -N4 and -N1 plus -N4 plus -N5, microsomal membrane proteins from adult heart (*h adult*, 50 μg), and protein lysate from heart of P7 mice (*h P7*, 100 μg) using the antibody 425 for CaVβ2. *, compare with legend in Fig. 1*C*.

cDNA was identified although the N2-coding exon 1B is present within the mouse *Cacnb2* gene. Supplemental Fig. S1 shows an alignment of the amino acid sequences derived from the four types of clones identified. They only differ in the N termini N1, N3, N4, and N5 whereas the remaining sequences starting with the amino acid residues GSA (exon 3, Fig. 2) are identical within the four CaVβ2 splice variants. The sequences following V1 comprise three serine residues, which in the rat CaVβ2-N3 orthologue have been suggested to be phosphorylated in the heart *in vivo* and *in vitro* (Ser-459, Ser-478, and Ser-479 in CaVβ2a-N3 (35)).

CaVβ2 Expression in Isolated Cardiac Myocytes

So far the results demonstrate expression of predominantly CaVβ2a-N4, CaVβ2a-N1, and CaVβ2a-N5 in murine heart. For construction of the cDNA libraries, poly(A)$^+$ RNA had been isolated from the entire heart; thus, RNA from fibroblasts, endothelial cells, and neurons was included. To refine the expression analysis, 10–12 cardiomyocytes from adult and embryonic hearts were subjected to combined cDNA synthesis and PCR reactions using primer pairs specific for N1-, N3-, N4-, and N5-type N termini. Analysis of the PCR products revealed that the CaVβ2-N1, -N4, and -N5 splice variants are expressed in adult and embryonic cardiomyocytes (Fig. 3). No PCR product was obtained for CaVβ2-N3 demonstrating that CaVβ2-N3 is not expressed in cardiomyocytes confirming the result obtained by cDNA library screening.

In Vitro Reconstitution of the in Vivo CaVβ2 Protein Expression Pattern

Considering that CaVβ2a-N1, CaVβ2a-N4, and CaVβ2a-N5 are expressed in cardiac myocytes, we wondered if these proteins are sufficient to explain the CaVβ2 protein pattern observed in Western blot experiments (Fig. 1*C*). Therefore, the three proteins were separately expressed in COS cells and lysates of these cells were used for Western blots (Fig. 4). As controls we used protein fractions from hearts of adult mice (Fig. 4, *h adult*) and of P7 mice (Fig. 4, *h P7*). The electrophoretic mobilities of CaVβ2a-N4 and CaVβ2a-N5 proteins expressed in COS cells (Fig. 4) resemble the mobility of the ~68-kDa CaVβ2 protein endogenously expressed in the adult heart (Fig. 4, *h adult*) and in the P7 heart (Fig. 4, *h P7*). In contrast, the CaVβ2a-N1 protein runs slightly slower (Fig. 4), very much like the ~72-kDa CaVβ2 protein endogenously co-expressed with the ~68-kDa CaVβ2 protein in the P7 heart. Apparently the N4- and N5-variants are the predominant CaVβ2 proteins expressed in the adult mouse heart, whereas in P7 hearts the CaVβ2a-N1 protein is additionally co-expressed. This assumption is supported by the finding that the protein patterns of mixtures of the respective COS cell lysates (Fig. 4) resemble the pattern observed in P7 hearts.

In summary, three CaVβ2 protein variants are expressed in mouse heart with CaVβ2a-N1 being expressed predominantly in embryonic stages, followed later by the additional expression of CaVβ2a-N4 and -N5, which become more and more the prevailing CaVβ2 proteins in the maturing heart.

Next we wanted to study the influence of these CaVβ2 proteins on LTCC currents (I_{Ca}). To keep the heterologous expression system as close to the murine Ca^{2+} channel as possible, we wanted to co-express only the cDNAs of the murine CaV1.2 and the CaVβ2 variants in HEK293 cells. No full-length murine cardiac CaV1.2 cDNA was available or obtainable, why we amplified murine full-length CaV1.2 cDNA from mouse heart (supplemental "Experimental Procedures," Fig. S2, and Table S6). The exons 1A and 1B are supposed to encode the N terminus of the cardiac (1A) and smooth muscle CaV1.2 (1B) proteins in rabbit (5, 36), rat, and human. Depending on the presence of either exon the CaV1.2 clones were referred to as CaV1.2a and CaV1.2b.

Different Modulation of L-type Ca^{2+} Channel Currents (I_{Ca}) by the CaVβ2 Variants

Current Density and Steady-state Activation and Inactivation—First, we analyzed current densities at different test potentials in HEK293 cells co-expressing CaV1.2a and each of the CaVβ2 variants. As controls we used non-transfected HEK293 cells and HEK293 cells just expressing CaV1.2a. Ca^{2+} currents were recorded in response to voltage steps of 400-ms duration to −70 mV up to +70 mV in 10-mV increments from a holding

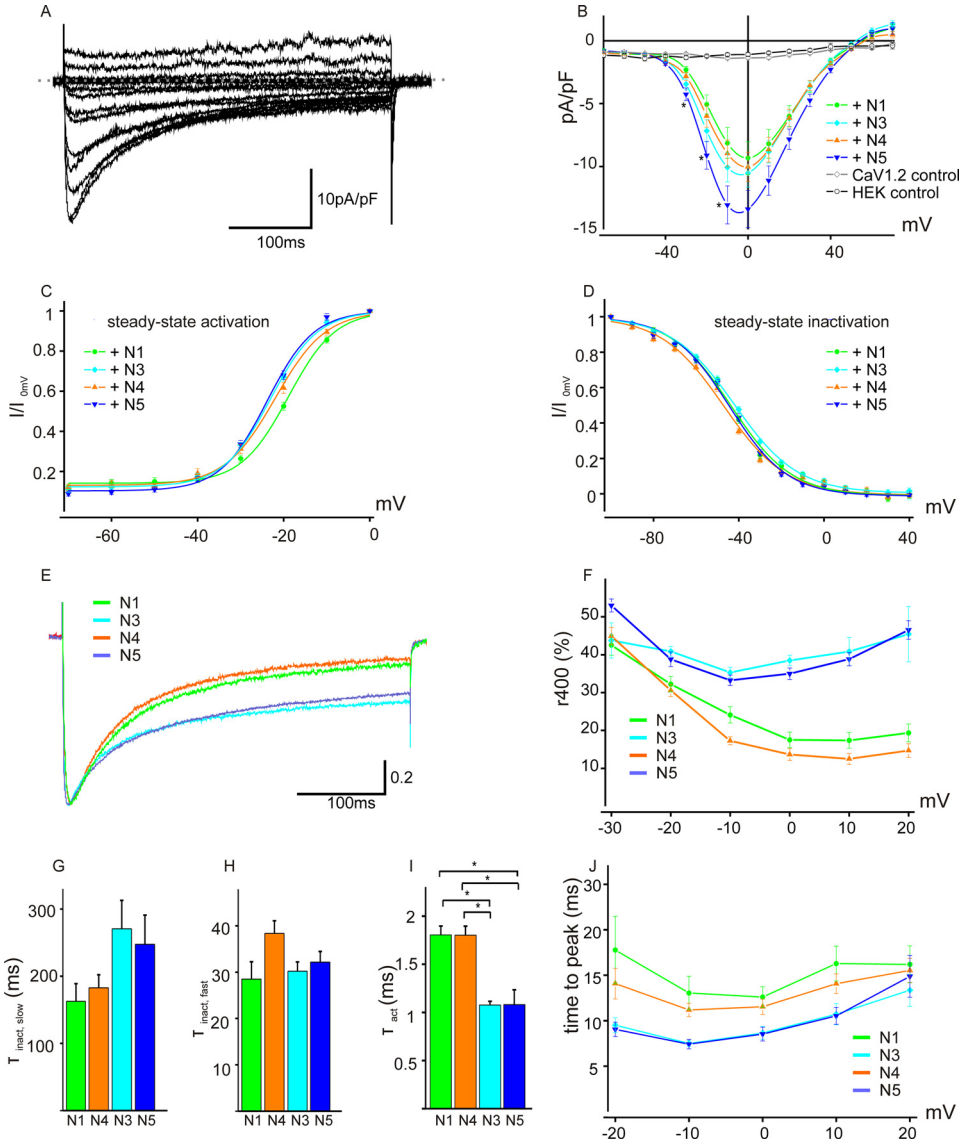

FIGURE 5. **Effects of CaVβ2 variants on I_{Ca}.** *A*, family of current traces obtained in CaV1.2a/CaVβ2a-N4 co-expressing cells in response to depolarizations from −70 mV up to +70 mV in 10 mV increments from a holding potential of −90 mV. *B*, averaged current-voltage relationships of I_{Ca} extracted from experiments as shown in Fig. 5*A*; *symbols* and *colors* are indicated. *Asterisks* indicate statistically significant differences ($p < 0.05$) between CaVβ2a-N1 and -N5. *HEK control*, non-transfected HEK293 cells; *CaV1.2 control*, HEK293 cells just expressing CaV1.2. *C*, steady-state activation; *D*, inactivation in the presence of CaVβ2a-N1 (*green*), -N3 (*cyan*), -N4 (*orange*), and -N5 (*blue*). Peak currents were normalized to the value at 0mV (for activation) and to the maximal I_{Ca} after a 5-s pulse to −100 mV (for inactivation). Curves were fitted with a single Boltzmann equation. *E–H*, inactivation of I_{Ca}. *E*, superimposed normalized mean I_{Ca} traces of cells co-expressing CaV1.2 plus CaVβ2a-N1, -N3, -N4, or -N5, respectively, showing that CaVβ2a-N1 and -N4 determine faster inactivation than CaVβ2a-N3 and -N5. *F*, analysis of the I_{Ca} remaining at the end of a 400-ms depolarization (r400) reveals CaVβ2 variant-specific differences in inactivation kinetics at test potentials ranging from −30 to +20 mV (10 mV increments used). *G* and *H*, time constants of slow ($\tau_{inact,slow}$) (*G*) and fast inactivation ($\tau_{inact,fast}$) (*H*) at 0-mV test potential. *I* and *J*, activation of I_{Ca}. *I*, time constants of $\tau_{activation}$ (τ_{act}) at the test potential of 0 mV are very similar for CaVβ2a-N1 and -N4 *versus* CaVβ2a-N3 and -N5, with the latter showing significantly faster activation kinetics. *J*, time to peak values also illustrate the similar effects of CaVβ2a-N1 and -N4 *versus* CaVβ2a-N3 and -N5 on I_{Ca} activation. Data are given as mean ± S.E. Numbers of cells used for the various current recordings: 15 to 28 (for details see supplemental Tables S2–S5).

potential of −90 mV. Fig. 5*A* shows a family of current traces in CaV1.2a/CaVβ2a-N4-expressing cells; the average current-voltage (I-V) relationships for the different co-expressions are shown in Fig. 5*B*. Recordings in HEK293 cells co-expressing CaV1.2a and a CaVβ2 protein reveal characteristic I_{Ca}, which were not observed in control HEK293 cells.

The I_{Ca} amplitude at 0 mV was in the range of −9.34 ± 1.31 pA/pF (CaVβ2a-N1, $n = 24$ cells) to 13.39 ± 1.48 pA/pF (CaVβ2a-N5, $n = 28$) indicating that current density is largest when the CaVβ2a-N5 is co-expressed; especially at negative potentials (−30 to −10 mV) there is a significant difference in comparison with currents elicited from cells co-expressing CaVβ2a-N1 ($p < 0.05$). Individual I-V relationships were fitted with a Boltzmann equation to obtain further information about the I_{Ca} properties (see supplemental Table S2 for summary). No significant differences in the apparent reversal potentials (E_{rev}) and in the maximal whole-cell conductances (G_{max}) were observed between the currents obtained from cells co-expressing CaV1.2a and CaVβ2a-N1 to -N5 (E_{rev} was in the range of 53.42 ± 1.66, $n = 28$ (CaVβ2-N3) to 58.37 ± 1.45 mV, $n = 26$ (CaVβ2a-N4); G_{max} at 0 mV was in the range of 0.18 ± 0.02, $n = 26$ (CaVβ2a-N4) to 0.26 ± 0.03nS/pF, $n = 28$ (CaVβ2a-N5)), whereas the voltage for half-activation $V_{1/2,act}$ was significantly different for cells co-expressing CaV1.2a with CaVβ2a-N1 (−16.91 ± 1.02 mV, $n = 24$) or CaVβ2a-N5 (−20.29 ± 0.79mV, $n = 28$, $p < 0.05$) (supplemental Table S2).

Steady-state activation and inactivation has been shown previously to be affected by the type of co-expressed CaVβ subunit in heterologous expression studies (37, 38). As shown in Fig. 5*C* there was a significant effect of CaVβ2a-N1 compared with CaVβ2a-N3, -N4, and -N5 on the steady state activation. The midpoint of activation, $V_{1/2,ss-act}$, of the normalized I-V curves was shifted to less negative potentials by co-expressing CaVβ2a-N1 compared with the co-expressed CaVβ2a-N3, -N4, and -N5 (CaVβ2a-N1, −18.96 ± 0.58 mV, $n = 24$; CaVβ2a-N3, −23.07 ± 0.47 mV, $n = 28$; CaVβ2a-N4, −21.96 ± 0.75 mV, $n = 26$; CaVβ2a-N5, −23.84 ± 0.57 mV, $n = 28$; with N1/N3 $p < 0.001$, N1/N4 $p < 0.01$, and N1/N5 $p < 0.001$) (Fig. 5*C* and supplemental Table S3). The half-maximal potential for inactivation, $V_{1/2,ss-inact}$ (Fig. 5*D*), was found to be different between

CaVβ2a-N4 (−47.05 ± 0.72, $n = 26$) and -N3 (−41.91 ± 0.71 mV, $n = 28$, $p < 0.001$), or -N1 (-43.47 ± 1.09 mV, $n = 24$; $p < 0.05$) (supplemental Table S3).

Kinetics of I_{Ca} Depend on the Type of Co-expressed CaVβ2

Inactivation Kinetics—There were obvious differences among the CaVβ2 variants on inactivation of I_{Ca} as can be seen by the normalization of the mean I_{Ca} traces for the various CaV1.2a/CaVβ2 combinations (Fig. 5*E*). Inactivation kinetics of I_{Ca} were faster in the presence of CaVβ2a-N1 or CaVβ2a-N4 than in the presence of CaVβ2a-N3 or CaVβ2a-N5; I_{Ca} from CaV1.2a/CaVβ2a-N3 and CaV1.2a/CaVβ2a-N5 channels inactivated with almost the same kinetics. Apparently, CaVβ2a-N1 and CaVβ2a-N4 as well as CaVβ2a-N3 and CaVβ2a-N5 comprise two groups, which confer distinct inactivation kinetics to I_{Ca}. This is also obvious when comparing the remaining I_{Ca} 400 ms (r400) after applying a test potential ranging from −30 to +20 mV (Fig. 5*F* and supplemental Table 4A). For currents elicited from CaV1.2a/CaVβ2a-N3 channels, r400 values changed only slightly in the voltage range from −30 mV (43.78 ± 4.62%) to +20 mV (45.42 ± 7.28%, $n = 28$). Currents elicited from CaV1.2a/CaVβ2a-N5 channels showed a similar behavior in the range from −20 to +20 mV, but resulted in a more pronounced drop of r400 values between −30 mV (53 ± 1.73%, $n = 28$) and +20 mV (46 ± 2.46%). In contrast, for currents obtained from CaV1.2a/CaVβ2a-N1 and CaV1.2a/CaVβ2a-N4 channels the r400 values markedly declined with increasing voltage from −30 to +20 mV (CaVβ2a-N1: from 42.52 ± 2.66% to 19.36 ± 2.33%, $n = 24$; CaVβ2a-N4: from 44.9 ± 2.32% to 14.68 ± 1.81%, $n = 26$) indicating a stronger voltage dependence of inactivation for CaV1.2a/CaVβ2a-N1 or -N4 channels than for CaV1.2a/CaVβ2a-N3 or -N5 channels, respectively. Inactivation of I_{Ca} followed bi-exponential kinetics and comparing the time constants of the slow inactivation ($\tau_{inact,slow}$) at 0 mV, the co-expressed CaVβ2a-N3 or CaVβ2a-N5 lead to pronounced slower inactivation of I_{Ca} than CaVβ2a-N1 or CaVβ2a-N4 (Fig. 5*G*). The time constants for fast inactivation ($\tau_{inact,fast}$) barely differed from each other although a slightly higher value was observed in the presence of CaVβ2a-N4 (Fig. 5*H*, supplemental Table S4B).

Activation Kinetics—Activation of I_{Ca} at 0 mV followed a single exponential fit and the resulting time constants (τ_{act}) differed significantly between CaVβ2a-N1 or CaVβ2a-N4, leading to slower activation kinetics, and CaVβ2a-N3 or CaVβ2a-N5 evoking faster channel activation kinetics (Fig. 5*I*) with τ_{act} values for CaVβ2a-N1 and CaVβ2a-N4 as well as for CaVβ2a-N3 and CaVβ2a-N5, respectively, being almost identical (supplemental Table S5A). Correspondingly, the time to peak values of I_{Ca} at 0 mV were larger for currents recorded from CaV1.2a/CaVβ2a-N1 and -N4 channels than for CaV1.2a/CaVβ2a-N3 or -N5 channels, respectively (Fig. 5*J*, supplemental Table S5B).

DISCUSSION

In a first series of experiments we show that CaVβ2 is the major CaVβ protein expressed in the adult mouse heart and that a switch of CaVβ2 protein isoform expression occurs during development.

Whereas numerous studies described cloning of Ca^{2+} channel subunits and Ca^{2+} channel composition in the human, guinea pig, and rat heart (5, 7, 25, 29, 39, 40, 41) the molecular "make-up" of the mouse cardiac LTCC is much less defined, although several mouse lines have been created with Ca^{2+} channel subunit transgenes as preclinical models for heart diseases (22, 23, 24, 42, 43).

CaVβ2 Protein Expression in Heart during Development—In the mouse heart, LTCCs are already functional at E9.5 (17). Analysis showed expression of the CaVβ2 protein throughout embryonic development whereas CaVβ1 and CaVβ4 protein expression was not detectable. The CaVβ3 protein is very weakly expressed in the embryonic hearts but not in hearts from perinatal and adult mice. We observed a switch in CaVβ2 protein expression from a ~72-kDa protein, mainly expressed at early embryonic stages to a ~68-kDa protein in hearts from adult mice.

Screening of cDNA Libraries for CaVβ2 Subunit Variants and Reconstitution of the CaVβ2 Protein Expression Pattern—To identify possible CaVβ2 variants we constructed cDNA libraries which were screened by probes covering the conserved domains C1 and C2 which together with V2 comprise the CaVβ2 core. Most groups (29, 30, 37, 44) used strategies aimed at the specific amplification of a DNA fragment to obtain CaVβ2 variants, which is critically determined by the primer pair used for PCR. In contrast, the screening of cDNA libraries represents a rather unbiased approach to identify which mRNA is expressed. In addition, this approach makes it possible to study the frequencies of given cDNAs, provided a sufficient number of clones are available. In the case of cardiac CaVβ2, sixty independent cDNA clones were identified, subcloned, and sequenced allowing an estimate of the types of CaVβ2 splice variants expressed in mouse heart and their naturally occurring frequencies. By this method, only potential CaVβ2 variants lacking the C1-V2-C2 core region (30) may have been missed. We confirmed the results by PCR amplification of the CaVβ2 variants identified by cDNA library screening using isolated cardiomyocytes as template. The combined approaches identified three CaVβ2 variants expressed in murine cardiomyocytes, CaVβ2a-N1, -N4, and -N5, which only differed in their V1 regions encoded by alternate exons. Reconstitution of the protein pattern of ~72- and ~68-kDa proteins *in vitro* by co-expression of CaVβ2a-N1, -N4, and -N5 can explain the protein pattern obtained in protein fractions from mouse heart at different developmental stages. CaVβ2a-N1 is predominantly expressed in hearts from embryonic and neonatal mice, whereas CaVβ2a-N4 and -N5 are isoforms expressed in hearts from neonatal and adult mice. The CaVβ2a-N1 protein is not detectable in protein fractions from adult heart. Results from cDNA library screening indicate a low number of CaVβ2 N1-type protein in the adult heart, which might have escaped detection with available antibodies.

The N2-type variant comprising the second protein-coding exon (exon 1B) was not identified at all. It encodes a twelve amino acid residues sequence (MDQASGLDRLKI), which is predicted to be alternatively spliced to the third protein coding exon (exon 2A); the orthologue exons have been identified in rat (rat CaVβ2c, GenBank™ Acc. No. AY190119) rabbit (rab-

bit cardiac CaVβ2b, Ref. 7) and human heart (CaVβ2-N2, Ref. 29). The N3-type variant was identified once among sixty clones but shown to be absent in cardiomyocytes. Consistent with our results, it seems to be neither expressed in rabbit heart (7, 26) nor, according to independent electrophysiological studies, in rat cardiomyocytes (33).

Modulation of I_{Ca} by the CaVβ2 Variants—In previous studies the impact of CaVβ2 proteins on I_{Ca} was primarily investigated by heterologously co-expressed channel subunits from different species (29, 37, 44). Here we wanted to reconstitute a murine LTCC channel in a heterologous expression system and co-expressed murine CaV1.2a with the murine CaVβ2 proteins identified before. The CaV$\alpha_2\delta$ subunit is known to predominantly affect LTCC function by increasing CaV1.2 channel density (45): It was not co-expressed, because it is not known precisely which of the four *Cacna2d* genes is expressed in murine cardiac myocytes (46).

The four CaVβ2a variants CaVβ2a-N1, -N3, -N4, and -N5 increased I_{Ca} density in a similar way with CaVβ2a-N5 causing the largest increase. Inactivation kinetics was accelerated in the presence of CaVβ2a-N1 and -N4 compared with the inactivation in the presence of CaVβ2a-N3 and -N5. Additionally, CaVβ2a-N1/-N4 caused slower I_{Ca} activation kinetics than CaVβ2a-N3/-N5. These results correspond to those reported with human CaVβ2a splice variants as well as to the observation that the four CaVβ2a variants form two functional groups (37).

Interestingly, the two splice variants, CaVβ2a-N1 and CaVβ2a-N4, which lead to unique steady-state inactivation/activation characteristics are the predominantly expressed variants in embryonic (CaVβ2a-N1) and adult (CaVβ2a-N4) mouse heart.

Role of Switch in Splicing Pattern for Murine Cardiac Development—Both CaV1.2/CaVβ2a-N1 and CaV1.2/CaVβ2a-N4 channels show fast inactivation kinetics but differ in voltage dependence of activation and inactivation. During mouse heart development, an increase of heart rate is observed with action potentials becoming shorter at the adult than at the embryonic, fetal, or neonatal stages (47). The plateau phase of the action potential is shaped in particular by the inactivation characteristics of I_{Ca}. Co-expression of CaV1.2/CaVβ2a-N4 resulted in a more hyperpolarizing shift compared with CaV1.2/CaVβ2a-N1, with the shift from CaVβ2a-N1 to -N4, suggesting it is important for the action potential inactivation properties during heart maturation.

CaVβ2a-N4 increased the fraction of channels activating at lower voltages compared with CaVβ2a-N1. CaVβ2a-N1 is the predominant isoform in embryonic heart and the latter finding may reflect that in early embryonic stages cardiac contraction requires intracellular Ca^{2+} oscillations rather than Ca^{2+} influx via L-type Ca^{2+} channels (48). It may also go in parallel with a decreased open probability and availability of single L-type Ca^{2+} channels, as observed in the presence of the human orthologue of CaVβ2a-N1 but not in the presence of CaVβ2a-N4 (44). Furthermore, at early embryonic stages, CaV1.3 and not CaV1.2 seem to be the predominantly expressed α1-subunit (49), so that CaV1.3 could interact with CaVβ2a-N1 in a different way than CaV1.2.

Acknowledgments—We thank Christine Wesely and Christin Matka for precious assistance; Susanne Stolz for initial experiments; Adolfo Cavalié for helpful discussions; Sabine Pelvay, Ramona Gölzer, and Martin Jung for immunizing and bleeding rabbits; Peter Lipp and Anne Vercerdea for providing the adult isolated cardiomyocytes.

REFERENCES

1. Reuter, H. (1983) *Nature* **301,** 569–574
2. Bers, D. M. (2002) *Nature* **415,** 198–205
3. Fabiato, A., and Fabiato, F. (1979) *Annu. Rev. Physiol.* **41,** 473–484
4. Catterall, W. A. (2000) *Annu. Rev. Cell Dev. Biol.* **16,** 521–555
5. Mikami, A., Imoto, K., Tanabe, T., Niidome, T., Mori, Y., Takeshima, H., Narumiya, S., and Numa, S. (1989) *Nature* **340,** 230–233
6. Groner, F., Rubio, M., Schulte-Euler, P., Matthes, J., Khan, I. F., Bodi, I., Koch, S. E., Schwartz, A., and Herzig, S. (2004) *Biochem. Biophys. Res. Commun.* **314,** 878–884
7. Hullin, R., Singer-Lahat, D., Freichel, M., Biel, M., Dascal, N., Hofmann, F., and Flockerzi, V. (1992) *EMBO J.* **11,** 885–890
8. Haase, H., Pfitzmaier, B., McEnery, M. W., and Morano, I. (2000) *J. Cell. Biochem.* **76,** 695–703
9. Pragnell, M., De Waard, M., Mori, Y., Tanabe, T., Snutch, T. P., and Campbell, K. P. (1994) *Nature* **368,** 67–70
10. Bichet, D., Cornet, V., Geib, S., Carlier, E., Volsen, S., Hoshi, T., Mori, Y., and De Waard, M. (2000) *Neuron* **25,** 177–190
11. Altier, C., Dubel, S. J., Barrère, C., Jarvis, S. E., Stotz, S. C., Spaetgens, R. L., Scott, J. D., Cornet, V., De Waard, M., Zamponi, G. W., Nargeot, J., and Bourinet, E. (2002) *J. Biol. Chem.* **277,** 33598–33603
12. Dolphin, A. C. (2003) *Pharmacol. Rev.* **55,** 607–627
13. Mitterdorfer, J., Froschmayr, M., Grabner, M., Striessnig, J., and Glossmann, H. (1994) *FEBS Lett.* **352,** 141–145
14. Walker, D., and De Waard, M. (1998) *Trends Neurosci.* **21,** 148–154
15. Hanlon, M. R., Berrow, N. S., Dolphin, A. C., and Wallace, B. A. (1999) *FEBS Lett.* **445,** 366–370
16. Cordeiro, J. M., Marieb, M., Pfeiffer, R., Calloe, K., Burashnikov, E., and Antzelevitch, C. (2009) *J. Mol. Cell Cardiol.* **46,** 695–703
17. Weissgerber, P., Held, B., Bloch, W., Kaestner, L., Chien, K. R., Fleischmann, B. K., Lipp, P., Flockerzi, V., and Freichel, M. (2006) *Circ. Res.* **99,** 749–757
18. Gregg, R. G., Messing, A., Strube, C., Beurg, M., Moss, R., Behan, M., Sukhareva, M., Haynes, S., Powell, J. A., Coronado, R., and Powers, P. A. (1996) *Proc. Natl. Acad. Sci. U.S.A.* **93,** 13961–13966
19. Murakami, M., Yamamura, H., Suzuki, T., Kang, M. G., Ohya, S., Murakami, A., Miyoshi, I., Sasano, H., Muraki, K., Hano, T., Kasai, N., Nakayama, S., Campbell, K. P., Flockerzi, V., Imaizumi, Y., Yanagisawa, T., and Iijima, T. (2003) *J. Biol. Chem.* **278,** 43261–43267
20. Namkung, Y., Smith, S. M., Lee, S. B., Skrypnyk, N. V., Kim, H. L., Chin, H., Scheller, R. H., Tsien, R. W., and Shin, H. S. (1998) *Proc. Natl. Acad. Sci. U.S.A.* **95,** 12010–12015
21. Burgess, D. L., Jones, J. M., Meisler, M. H., and Noebels, J. L. (1997) *Cell* **88,** 385–392
22. Grueter, C. E., Abiria, S. A., Dzhura, I., Wu, Y., Ham, A. J., Mohler, P. J., Anderson, M. E., and Colbran, R. J. (2006) *Mol. Cell* **23,** 641–650
23. Chen, X., Zhang, X., Kubo, H., Harris, D. M., Mills, G. D., Moyer, J., Berretta, R., Potts, S. T., Marsh, J. D., and Houser, S. R. (2005) *Circ. Res.* **97,** 1009–1017
24. Jaleel, N., Nakayama, H., Chen, X., Kubo, H., MacDonnell, S., Zhang, H., Berretta, R., Robbins, J., Cribbs, L., Molkentin, J. D., and Houser, S. R. (2008) *Circ. Res.* **103,** 1109–1119
25. Perez-Reyes, E., Castellano, A., Kim, H. S., Bertrand, P., Baggstrom, E., Lacerda, A. E., Wei, X. Y., and Birnbaumer, L. (1992) *J. Biol. Chem.* **267,** 1792–1797
26. Qin, N., Platano, D., Olcese, R., Costantin, J. L., Stefani, E., and Birnbaumer, L. (1998) *Proc. Natl. Acad. Sci. U.S.A.* **95,** 4690–4695
27. Massa, E., Kelly, K. M., Yule, D. I., MacDonald, R. L., and Uhler, M. D. (1995) *Mol. Pharmacol.* **47,** 707–716
28. Allen, T. J., and Mikala, G. (1998) *Pflugers Arch.* **436,** 238–247

29. Foell, J. D., Balijepalli, R. C., Delisle, B. P., Yunker, A. M., Robia, S. L., Walker, J. W., McEnery, M. W., January, C. T., and Kamp, T. J. (2004) *Physiol. Genomics* **17,** 183–200
30. Harry, J. B., Kobrinsky, E., Abernethy, D. R., and Soldatov, N. M. (2004) *J. Biol. Chem.* **279,** 46367–46372
31. Kaestner, L., and Lipp, P. (2007) *Proc. of SPIE* **6633,** 66330K
32. Pearson, H. A., and Dolphin, A. C. (1993) *Pflugers Arch.* **425,** 518–527
33. Colecraft, H. M., Alseikhan, B., Takahashi, S. X., Chaudhuri, D., Mittman, S., Yegnasubramanian, V., Alvania, R. S., Johns, D. C., Marbán, E., and Yue, D. T. (2002) *J. Physiol.* **541,** 435–452
34. Chien, A. J., Carr, K. M., Shirokov, R. E., Rios, E., and Hosey, M. M. (1996) *J. Biol. Chem.* **271,** 26465–26468
35. Gerhardstein, B. L., Puri, T. S., Chien, A. J., and Hosey, M. M. (1999) *Biochemistry* **38,** 10361–10370
36. Biel, M., Ruth, P., Bosse, E., Hullin, R., Stühmer, W., Flockerzi, V., and Hofmann, F. (1990) *FEBS Lett.* **269,** 409–412
37. Takahashi, S. X., Mittman, S., and Colecraft, H. M. (2003) *Biophys. J.* **84,** 3007–3021
38. Jones, L. P., Wei, S. K., and Yue, D. T. (1998) *J. Gen. Physiol.* **112,** 125–143
39. Tang, Z. Z., Liang, M. C., Lu, S., Yu, D., Yu, C. Y., Yue, D. T., and Soong, T. W. (2004) *J. Biol. Chem.* **279,** 44335–44343
40. Ding, S., Kuroki, S., Kameyama, A., Yoshimura, A., and Kameyama, M. (1999) *J. Biochem.* **125,** 750–759
41. Tang, Z. Z., Liao, P., Li, G., Jiang, F. L., Yu, D., Hong, X., Yong, T. F., Tan, G., Lu, S., Wang, J., and Soong, T. W. (2008) *Biochim. Biophys. Acta* **1783,** 118–130
42. Hullin, R., Matthes, J., von Vietinghoff, S., Bodi, I., Rubio, M., D'Souza, K., Friedrich, Khan, I., Rottländer, D., Hoppe, U. C., Mohacsi, P., Schmitteckert, E., Gilsbach, R., Bünemann, M., Hein, L., Schwartz, A., and Herzig, S. (2007) *PLoS. ONE.* **2,** e292
43. Muth, J. N., Yamaguchi, H., Mikala, G., Grupp, I. L., Lewis, W., Cheng, H., Song, L. S., Lakatta, E. G., Varadi, G., and Schwartz, A. (1999) *J. Biol. Chem.* **274,** 21503–21506
44. Herzig, S., Khan, I. F., Gründemann, D., Matthes, J., Ludwig, A., Michels, G., Hoppe, U. C., Chaudhuri, D., Schwartz, A., Yue, D. T., and Hullin, R. (2007) *FASEB J.* **21,** 1527–1538
45. Davies, A., Hendrich, J., Van Minh, A. T., Wratten, J., Douglas, L., and Dolphin, A. C. (2007) *Trends Pharmacol. Sci.* **28,** 220–228
46. Gong, H. C., Hang, J., Kohler, W., Li, L., and Su, T. Z. (2001) *J. Membr. Biol.* **184,** 35–43
47. Wahler, G. M., Dollinger, S. J., Smith, J. M., and Flemal, K. L. (1994) *Am. J. Physiol.* **267,** H1157–H1166
48. Viatchenko-Karpinski, S., Fleischmann, B. K., Liu, Q., Sauer, H., Gryshchenko, O., Ji, G. J., and Hescheler, J. (1999) *Proc. Natl. Acad. Sci. U.S.A.* **96,** 8259–8264
49. Takemura, H., Yasui, K., Opthof, T., Niwa, N., Horiba, M., Shimizu, A., Lee, J. K., Honjo, H., Kamiya, K., Ueda, Y., and Kodama, I. (2005) *Circ. J.* **69,** 1405–1411